

Supporting Information

Hysteretic Adsorption and Desorption of Hydrogen by Nanoporous Metal-Organic Frameworks

Xuebo Zhao§, Bo Xiao§, Ashleigh J. Fletcher§, K. Mark Thomas§*Darren Bradshaw†, and Matthew J. Rosseinsky†

§Northern Carbon Research Laboratories, School of Natural Sciences, Bedson Building, University of Newcastle upon Tyne, Newcastle upon Tyne, NE1 7RU, UK;

† Department of Chemistry, University of Liverpool, Liverpool, L69 7ZD, UK.

Methods

The adsorption/desorption characteristics were studied using a Hiden Analytical Intelligent Gravimetric Analyser, which is an ultra high vacuum, clean system, with ultra pure (Air Products, 99.9999%) hydrogen and deuterium (BOC, 99.98% D₂). This system was suitable for the measurement of adsorption kinetics in porous materials.^(3,4,18,23) The microbalance had a long-term stability of $\pm 1 \mu\text{g}$ with a weighing resolution of $0.2 \mu\text{g}$. The approach to equilibrium was measured in real time using a computer algorithm. The pressure was monitored by three pressure transducers with ranges 0-0.002, 0-0.1 and 0-10 bar and maintained at the set point by active computer control of inlet/outlet valves throughout the duration of the adsorption kinetic experiments. The accuracy of the set-point pressure regulation was $\pm 0.02\%$ of the range used. Isotherms were measured to 16 bar H₂ pressure on **C** on a similar system equipped with a liquid nitrogen cryotrap on the inlet gas line at -196°C, -78°C and 22°C – the data were exactly comparable with those reported in the main body of the paper (Figure S2).

The measurement protocols used in this study were validated by the following experiments. Adsorption isotherms for D₂ on **AC** and **E** at -196°C gave ~2x the mass uptake and showed the same hysteresis characteristics as the corresponding hydrogen adsorption isotherms. The complete desorption of H₂ and the absence of hysteresis in the isotherms measured for **AC** and **C** also validate the measurement protocols used here. The validity of the uptake measurements was further confirmed by the temperature-dependent isobar data on these materials. The isobars were measured by firstly allowing the sample to equilibrate in hydrogen at 1 bar pressure at -196°C. The sample was then

heated at a rate of $0.3^{\circ}\text{C min}^{-1}$ at 1 bar hydrogen pressure and the mass adsorbed was monitored. The data were corrected for changes in buoyancy effects as a function of temperature. Thermodynamic analyses (Figures S3 – S6) and repeatability measurements (Figures S7 and S8) are outlined below to demonstrate the reliability of the protocols used here.

Materials Used and Preparation of the Adsorbents

All solvents, metal salts and ligands were used as received from the Aldrich Chemical Co. unless stated in parenthesis within the text. All of the procedures below have been previously outlined in references 17 – 20, 23 in the manuscript.

Synthetic Methods

Synthesis of **M and **E**:**

$\text{Ni}(\text{NO}_3)_2 \cdot 6\text{H}_2\text{O}$ (348 mg, 1.2 mmol) and 4,4'-bipyridyl (186 mg, 1.2 mmol) are each dissolved in 6 mL of methanol or ethanol, for the preparation of **M** and **E** respectively, such that the solutions are 0.2 M concentration. 2 mL portions of each solution are placed in opposite arms of an H-cell, and fresh alcohol carefully layered on top so as to completely fill the cell. Each cell is sealed with laboratory film and left to stand undisturbed at room temperature. After approximately three weeks single crystals of **M** or **E**, suitable for single crystal x-ray diffraction, are formed. Total yield = 280 mg (30%).

Synthesis of **C:**

$\text{Ni}(\text{NO}_3)_2 \cdot 6\text{H}_2\text{O}$ (218 mg, 0.75 mmol) and 1,3,5-benzenetricarboxylic acid (105 mg, 0.5 mmol) (btc) are gently warmed in 10 mL of resolved 1,2-propanediol (1,2-pd) [Avocado] until complete dissolution occurs. This stock solution is split into five equal portions and placed into 75 x 25 mm glass sample vials. Into each is placed a smaller sample vial, with a pierced lid, containing 5 drops of neat 3-picoline (3-pic). The larger vial is capped and sealed with laboratory film. The chiral crystalline phase grows after approximately three weeks. Yield = 450 mg (39%).

The samples were activated by removing the guests from the pores under high vacuum (2×10^{-10} bar) at 22°C using the Hiden Intelligent Gravimetric Analyzer (IGA; outgassing was typically carried out overnight at elevated temperatures depending on the stability of the material and stopped when a constant mass had been reached. Materials **M**, **E** and **C**

lose 7.7, 10.5 and 39 wt% of their mass respectively, upon outgassing, which is consistent with the calculated number of guests from elemental analysis and crystallographic studies.

Verification of Structure

The structural integrity of all adsorbents were verified, prior to activation and hydrogen uptake, by x-ray powder diffraction measurements using a Stoe Stadi-P diffractometer with a linear position-sensitive detector and monochromatic Cu K $_{\alpha 1}$ radiation. Data were recorded in the angular range $3 \leq 2\theta \leq 40^\circ$ in transmission geometry.

Supporting Information

Table S1. Porous Structure Characterisation Data

Material	Window Size /Å	Pore Cavity Cavity Size /Å	Total Pore Volume/ cm ³ g ⁻¹
AC	-	-	0.44
E	2.32 x 2.75	5.4 x 5.2 x 4.1	0.149
M	2.5 x 4.9	4.3 x 5.3 x 8.3	0.181
C	8.5 x 8.5	13.7 x 10.7	0.63

The total pore volumes for **AC** and **C** were obtained from the amount of N₂ adsorbed at $p/p^0 = 1$ at -196°C. The total pore volumes were obtained from methanol adsorption at 0°C. The micropore volume of **AC** obtained from carbon dioxide adsorption at 0°C by extrapolation of the Dubinin-Radushkevich equation was 0.18 cm³ g⁻¹.

Table S2: Crystallographic and Pore Structure Characterisation Parameters

Material ^a	H ₂ per F.U.	V _{ACC} (Å ³ /cell) ^c	Acc fraction (V _{ACC} /V _{CELL})	V _{OCC} (Å ³ /cell) [‡]	Occ fraction (V _{OCC} /V _{ACC})
C	4.1 [†]	10578	0.475	1065.3	0.100
C ^b	14.3 [†]	10578	0.475	3720.7	0.351
E	2.69*	793.8	0.201	348.9	0.440
M	4.11 *	1839.9	0.23	1064.3	0.578

a measurements at -196°C and 1 bar

b -196°C and 14 bar (Figure S1)

c accessible pore volume(V_{ACC}) results from PLATON (Spek, A; Acta Crystallogr, Sect A 1990, 46, C34)

* these values based on fitting of the Langmuir equation

[†] these values based on total uptake value from the measured isotherm data

[‡] The volume occupied (V_{OCC}) is calculated from the liquid density and close packing of 32.2 Å³, measured at the triple point. For comparison, the large pore material MOF-5 has an occupied fraction of 0.137 at 1 bar and -196°C when calculated in this way.¹¹

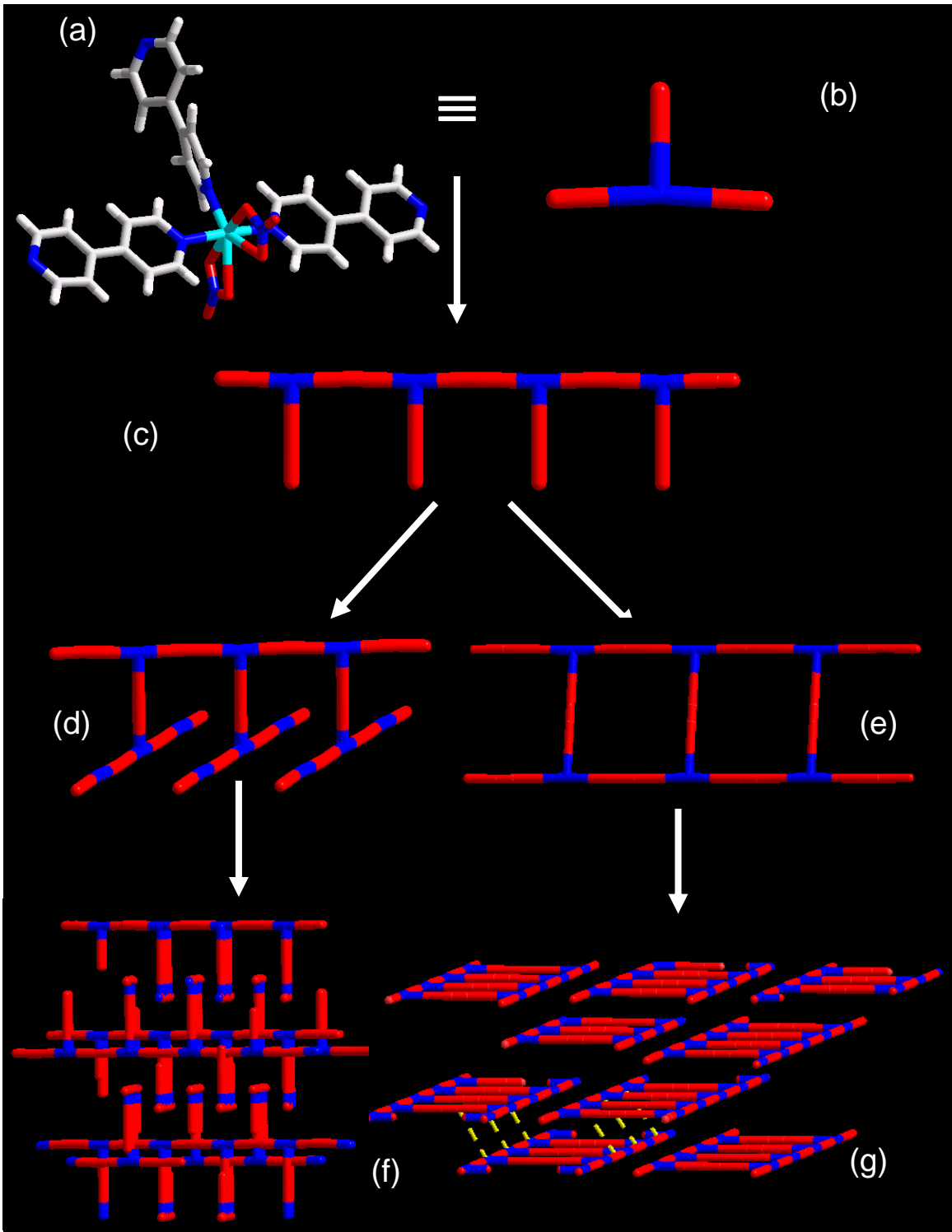


Figure S1. The coordination of the Ni site in both $\text{Ni}_2(\text{bipy})_3(\text{NO}_3)_4$ polymorphs of three bipy and two nitrate groups (a) produces a “T” –shaped node (b) that assembles into a one-dimensional chain (c). These chains are assembled by linking via the “cross” of the T either parallel to each other (e, g) (CH_3OH structure) to give one-dimensional ladders or perpendicular to each other (d, f) to give interlocking two-dimensional bilayers when grown from ethanol. The non-classical C-H...O interactions responsible for the thermal stability of the CH_3OH structure are shown as broken yellow lines in (g).

High-pressure H_2 isotherms for porous metal organic framework C:

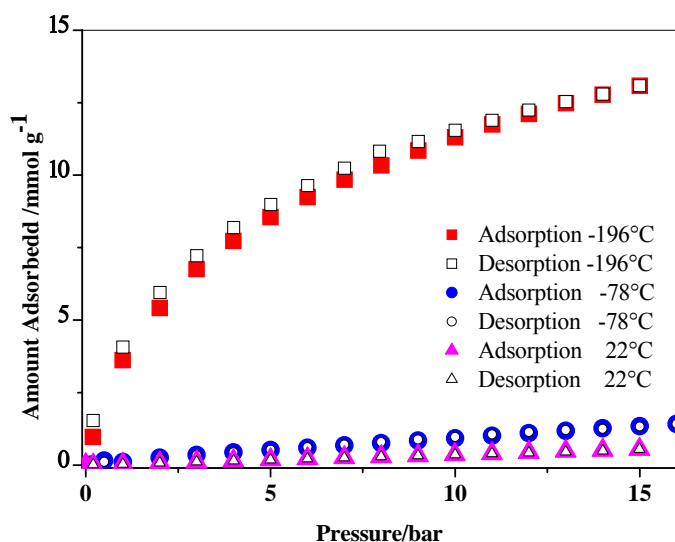


Figure S2: High-pressure H_2 adsorption(closed symbols) and desorption(open symbols) isotherms on the larger pore metal organic framework C at -196°C , -78°C and 22°C .

The low uptakes of H_2 by C at -78°C and 22°C compared with -196°C , even at pressures up to 16 bar, are consistent with the observation that virtually no adsorption is seen above $\sim -130^\circ\text{C}$ in the isobar measurements shown in Figure 4 of the manuscript.

Hydrogen Sorption Isotherms and Thermodynamic treatment for AC

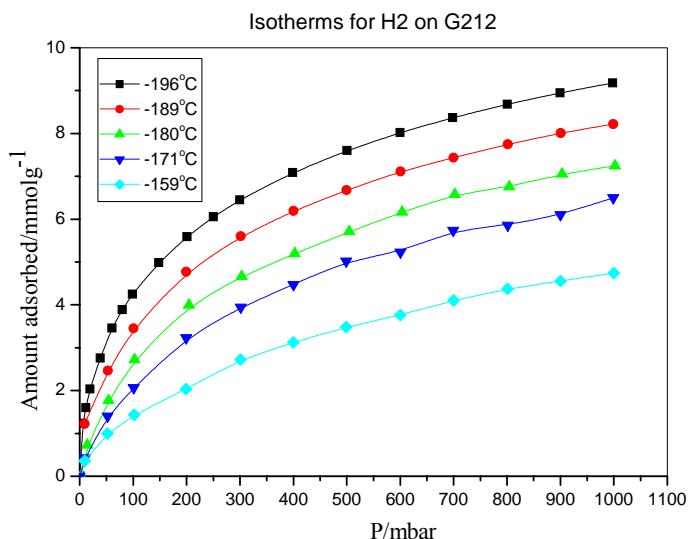


Figure S3 Isotherms for hydrogen adsorption on AC: Temperature Range: -196 – -159°C
All the isotherms are Type 1 in the IUPAC Classification Scheme

Virial Equation

A saturated vapor pressure is not available under supercritical conditions and hence it is more difficult to compare isotherms over a range of temperatures.

The virial equation can be written in the form

$$\ln(n/p) = A_0 + A_1 n + A_2 n^2 \text{ ---- (1)}$$

where n is the amount adsorbed at pressure p and the first virial coefficient A_0 is related to the Henry's law constant K_0 by the equation $K_0 = \exp(A_0)$. K_0 is dependent on the interaction between the adsorbent surfaces and the adsorbed gas molecules. In this study analysis of the data showed that the higher terms (A_2 etc) in the virial equation could be ignored under conditions of low surface coverage. The virial graphs for all the temperatures studied were clearly linear (see Figure S4). The values of the first virial coefficient (A_0) reflect adsorbate adsorbent interaction whereas the second virial parameter A_1 is a function of adsorbate-adsorbate interactions. The value for the isosteric

heats of adsorption (Q_{st}) at zero surface coverage can be obtained from a graph of A_0 versus $1/T$.

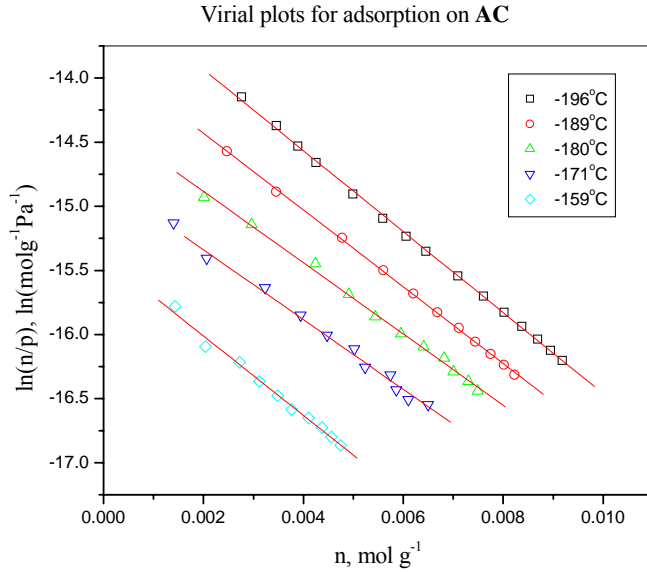


Figure S4. Virial graphs for the adsorption of hydrogen on **AC**: Temperature range: -196 – -159°C

The values of the second virial parameter (A_1) were typically $\sim 300 \text{ g mol}^{-1}$. These values are similar to those found for adsorption of oxygen, argon etc on carbon molecular sieves. (C.R.Reid, I.P. Okoye, K.M. Thomas *Langmuir*, **14**, 2415-2425 (1998).

Variation of Hydrogen Adsorption as a function of temperature

The change in the integral heat of adsorption Q with temperature can be described by the following equation:

$$\frac{dQ}{dT} = n_s (Cp_G - Cp_s) \tag{2}$$

where n_s is the amount adsorbed, Cp_G is the molar heat capacity of the gas phase at constant pressure, Cp_s is the molar heat capacity of the adsorbed phase and T is the temperature. Therefore, at zero surface coverage the enthalpy of adsorption is constant. The isosteric heats of adsorption (Q_{st}) at zero surface coverage can be obtained from the gradient of the graph of the first virial coefficient (A_0) versus $1/T$ (see Figure S5).

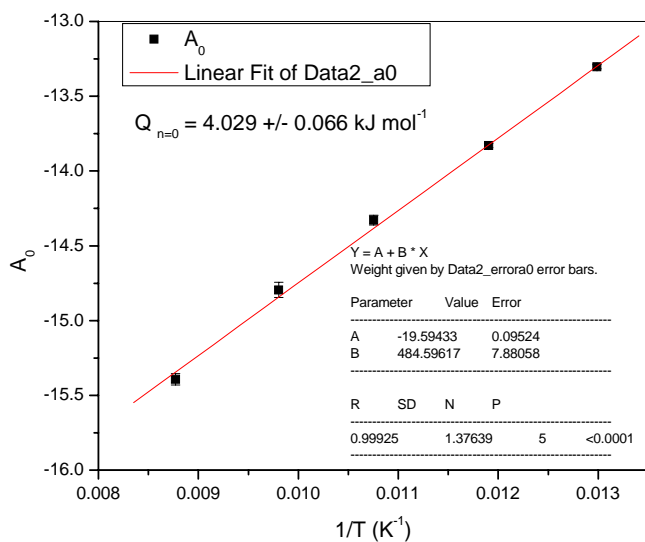


Figure S5. A graph of A_0 versus $1/T$ for hydrogen adsorption on **AC**

It is evident that the graph of A_0 versus $1/T$ is a straight line within experimental error indicating that the measurements are consistent with the thermodynamic prediction of constant enthalpy of adsorption at zero surface coverage.

The enthalpies of adsorption can also be calculated for a specific surface coverage using the Vant Hoff isochore (Figure S6)

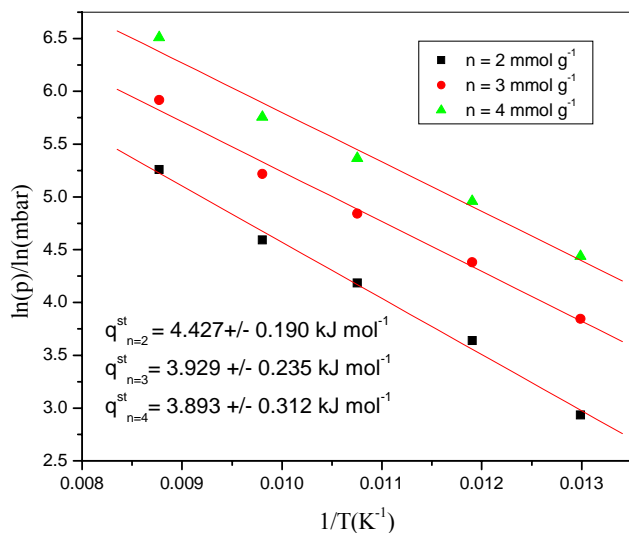


Figure S6. The variation of $\ln(p)$ versus $1/T$ for the adsorption of hydrogen on **AC**: Temperature range : -196 to -159°C

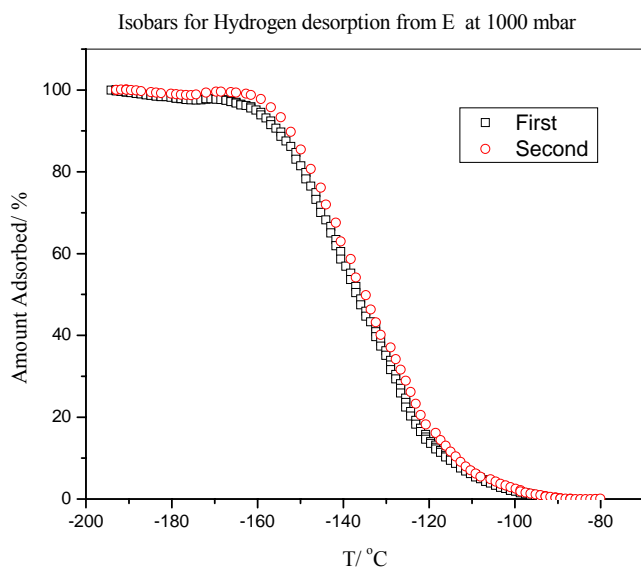
Summary of Thermodynamic Data for hydrogen adsorption on AC

Surface Coverage /mmol g ⁻¹	ΔH /kJ mol ⁻¹	Method
0	4.03 ± 0.07	Virial Equation
2	4.43 ± 0.19	Van't Hoff isochore
3	3.93 ± 0.24	“
4	3.89 ± 0.31	“

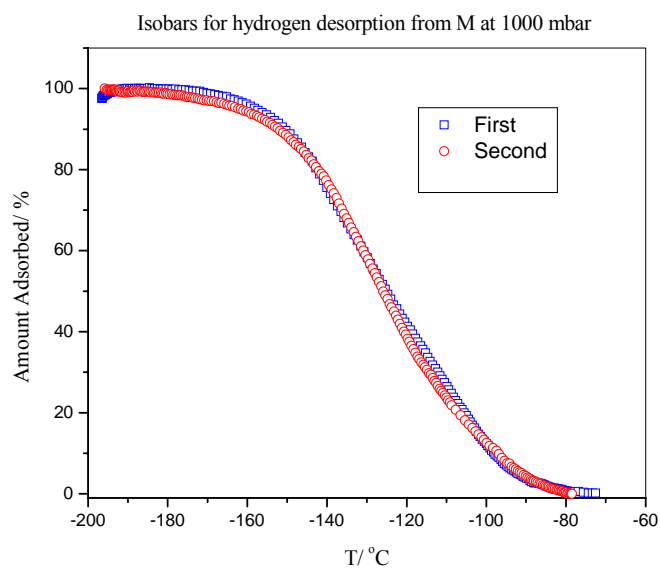
These values of the enthalpy of adsorption at various surface coverages derived from both methods are equal within experimental error. It is apparent that adsorption of hydrogen on activated carbon has a very low enthalpy of adsorption. The above results validate the measurement protocols used in this study.

Isobar Repeatability Measurements

a)



b)



c)

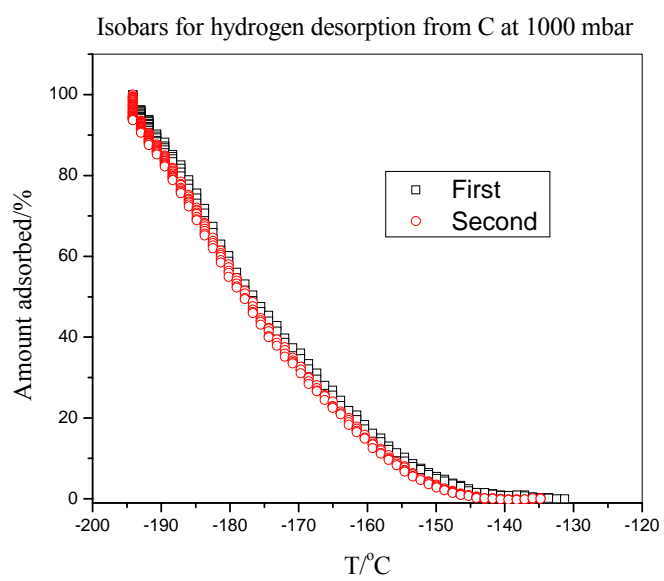


Figure S7. Isobar repeatability Tests a) **E**, b) **M** c) **C**

It is evident from Figure S7 that the isobars are repeatable and this validates the experimental protocol.

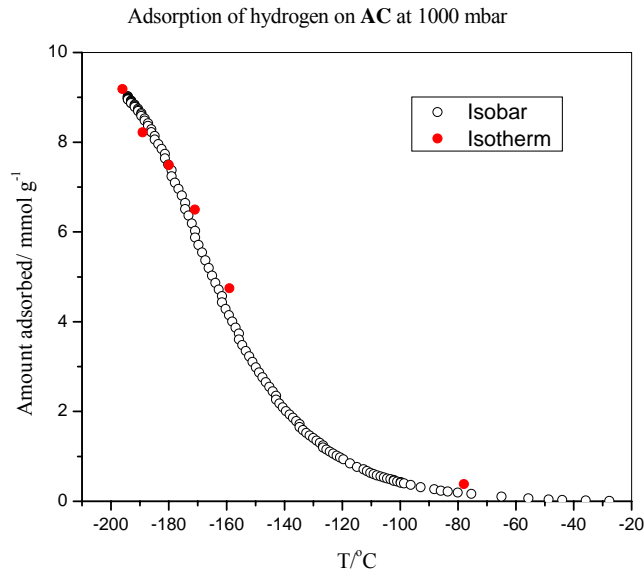


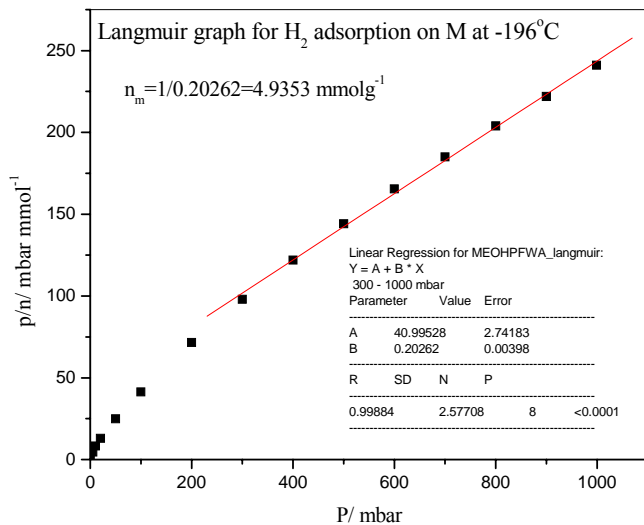
Figure S8. A comparison of the desorption isobar and adsorption isotherm data for adsorption of hydrogen on AC

It is apparent from Figure S8 that there is good agreement between the isotherm (Figure S3) and isobar data.

Langmuir Graphs

The estimates of the maximum amounts of hydrogen adsorbed on **E** and **M** were obtained from the Langmuir graphs given below.

a)



b)

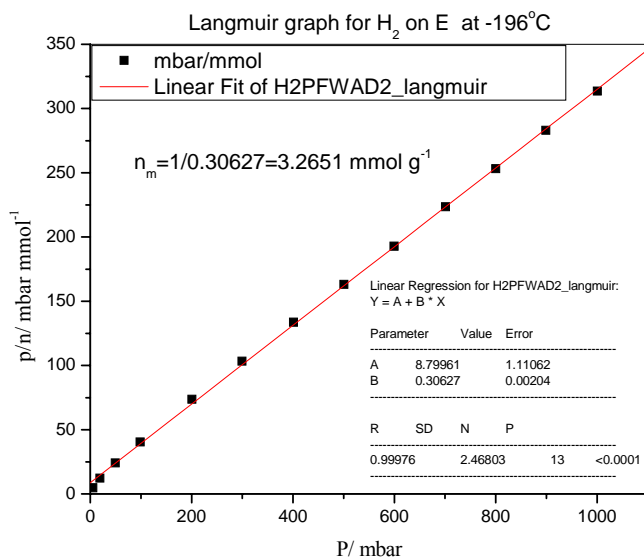


Figure S9. Langmuir graphs for the adsorption of hydrogen at -196°C on a) **M** and b) **E**